J Mater Sci (2006) 41:7459–7465
DOI 10.1007/s10853-006-0801-5

Effects of microballoons' size and content in epoxy on compressive strength and modulus

Kishore · Ravi Shankar · S. Sankaran

Received: 15 June 2005 / Accepted: 1 December 2005 / Published online: 20 September 2006

Abstract Five slabs containing volume of microballoons ranging from 33.4 to 51.5% and all belonging to a size range of 65–100 μm were made. In order to study the effect of size range, another slab, but belonging to a broader range of 44–175 μm, was also cast, where in the microballoons' content was 40.1% by volume. The first set of five slabs showed a decrease in compressive strength from 82.4 to 58 MPa as the microballoons' content increased. A similar trend was observed for modulus values also. The work further showed that the samples from the narrower size range display a higher strength. Microscopic examinations revealed crushing of microballoons for the highest microballoons' case while for the least microballoons bearing sample, deformation marks were visible on the epoxy matrix.

Introduction

Developments in the area of polymer based materials lead to the emergence of newer engineered systems. One such system is the syntactic foam, which is formed by mixing hollow microspheres (i.e., microballoons) in a binder matrix. Large number of choices for the polymeric matrices [1–3] and for hollow microspheres [4–7] make the topic a very interesting one to explore. The low density and controllable porosity of microballoons leads to attractive mechanical properties, which include specific, impact, shear and tensile strengths, as well as dynamic mechanical properties [8–14].

The studies on syntactic foams include one on elastic behavior [15] and another on theoretical and experimental aspects of characterization of foams [16]. Published report on physical characterization of foams [17] is also available. Other than the matrix system, among the key factors that determine the mechanical properties of syntactic foams, mention may be made of distribution of sizes, shape, strength, surface defects, surface treatments, volume (vol.)% and wall thickness of microballoons [18–28]. Literature on the effect of wall thickness [21, 23, 29], vol.%, and surface treatment of microballoons on mechanical properties of syntactic foams can be cited [30, 31]. Gupta et al. studied the effect of specimen aspect ratio on compressive response of syntactic foams [18]. The importance of wall thickness as a parameter to change the density, keeping the volume fraction of hollow particles constant, has been stressed after a consideration of compression data in another report [26]. Data on the compressive properties of syntactic foams for flat-wise and edgewise specimens' orientations are also available [23]. In one study, the facts that fracture toughness, K_{Ic} and the linear elastic energy release rate, G_{Ic}, increased with volume fraction of microspheres were established [14]. Based on the results of an

Kishore (✉)
Polymer Composites Laboratory, Centre for Advanced Studies, Department of Metallurgy, Indian Institute of Science, Bangalore 560 012, India
e-mail: balkis@met.iisc.ernet.in

R. Shankar
Fiber & Polymer Science, Materials Science and Engineering, College of Textiles, NC State University, 2401 Research Drive, Box 8301, Raleigh, NC 27695, USA

S. Sankaran
Aeronautical Development Establishment, New Thippasandra PO, Bangalore 560 075, India

experimental study on high strain rate compressive behavior of an epoxy syntactic foam, a constitutive model with strain rate and damage effects was developed in yet another effort [13]. In some of the recent studies the compressive response of syntactic foams, reinforced with fiber, was investigated [22, 28]. A fact that emerges out after considering all the above-mentioned investigations is that the issue of effect of size distribution of microballoons on the mechanical properties of syntactic foams has not been looked into in any detail till date. Further on, generally stated, the published reports deal with the characterization of compression behavior in three-phase syntactic foams [18–28, 32–35]. However, reports become scantier when a search for literature dealing with two-phase syntactic foams and their compression behavior is made. As, syntactic foams find applications in sub-sea equipments and under water vehicles, the study of the dependence of compression behavior on the level and size distribution of fillers has gained importance. Owing to these gaps found in the published reports an effort was made to fill the same where the objective, was two-fold, namely, to investigate first, the effect of content of microballoons on compressive strength, modulus, and fracture features and then to study the effect of size distribution of microballoons on the strength and modulus values.

Experimental

Materials

All the syntactic foams were prepared by using glass hollow microballoons as fillers and epoxy resin as matrix. Resin system used is Araldite LY-556 (Bisphenol-A Diglycidyl ether) and hardener HT-972 (aromatic amine). Resin and hardener were mixed in the ratio of 100:27 by weight. Epoxy resin, with an EEW value of 190, as specified by the manufacturer, is supplied by Vantico Performance Polymers Pvt. Ltd. The density of the cured resin system, determined experimentally, was 1180 kg/m^3. Glass hollow microspheres (called glass microballoons), Ecospheres SI, was supplied by Grace Electronic Materials, Belgium. Density of the glass microballoons was 250 kg/m^3. Size distribution of the microballoons was obtained by using Malvern Mastersizer particle size analyzer, the data from which are given later. Microballoons, used here, were chosen in the diameter ranges of 65–100 μm and 44–175 μm having a mean diameter of 82 μm and 109 μm, respectively, for making the two-phase syntactic foams.

Materials processing

To get a narrower distribution of microballoons sizes (i.e., 65–100 μm), microballoons were sieved inside a specially designed chamber. Syntactic foams slabs were fabricated by varying the volume percent of microballoons. Weighed quantities of resin and hardener, respectively, were mixed in a beaker by stirring and then heated to 95 °C. Predetermined quantity of microballoons was gradually added to this resin mixture while stirring the contents gently so that breakage of hollow microballoons can be minimized. The slurry was filled into a metallic mould of dimension 150 mm × 150 mm × 25 mm.

The cast syntactic foam slabs were cured at room temperature for 24 h and then cured first at 100 °C for 4 h and then at 160 °C for 3 h. In order to achieve the first objective of the present study (i.e., to see the effect of microballoons content on strength), five different syntactic foams slabs keeping the microballoons size in the range 65–100 μm, and labeled SF 01 to 05 in this work, were fabricated. Microballoons' content of each cast slab was later determined by burn out test, performed on the test coupons, the findings of which are listed in Table 1.

To accomplish the second objective of the present investigation (i.e., to study the effect of size distribution on strength), a syntactic foam slab (abbreviated SF 06) having a nominal value of about 42 vol.% of microballoons, corresponding to the SF 03 slab listed in Table 1, but now in the size range 44–175 μm, was scheduled for casting by the aforementioned procedure. However, after the casting was completed (designated SF 06 as stated earlier on), random burn out tests revealed the actual microballoons' content to be 40.1 vol.% which composition was different from all the cast slabs mentioned earlier on (i.e., SF 01 to 05, Table 1). The burn out tests data on SF 06, listed also in Table 1, indicate that a difference in the planned and the actual microballoons content for the cast slab has occurred. The small difference, could originate from factors like degree of mixing owing to a difference in the size range,

Table 1 Details of the syntactic foam slabs

Foam designation	Volume % of microballoons	Density of the cast slab (kg/m^3)
SF 01[a]	33.4	877
SF 02[a]	35.5	857
SF 03[a]	41.9	798
SF 04[a]	48.3	738
SF 05[a]	51.5	708
SF 06[b]	40.1	768

Size range for [a] 65 – 100 μm and [b] 44 – 175 μm

settling rate, viscosity of medium, etc. This variation of microballoons, from the nominal value for slab SF 06, added another experimental variable in the present study. How this factor is taken into account is covered later on in the results and discussion section. It must be stated at this juncture, that as two-phase foams was aimed at and made the aspect of open cell porosity is not considered in this work.

Compression test

Compression tests were performed at room temperature in a servo-hydraulic, computer controlled testing machine, namely, DARTEC 9500 at a constant strain rate of 0.01 s^{-1}. Specimens conforming to the ASTM 1621-73 specification [36] having dimension 15 × 15 × 7.5 mm were made for this purpose.

Particle size analysis of microballoons

Particle size distribution was determined by the Malvern make laser particle size analyzer (Fig. 1). The average particle size, given as numerical data by the analyzer, is about 78 μm. About 70% of the particles lie in the range of 65–100 μm with an average particle size of 82 μm.

Microscopy

The failed samples from uniaxial compression tests were examined in a JEOL make JSM 840A SEM to observe the fractographic features. Fractured samples were gold coated in a sputtering unit at a current of 10 mA, prior to mounting in SEM.

Results and discussion

Mechanical data

Effect of volume percent of microballoons

Table 2 lists the average strength values of the five replicate samples machined from the five different (i.e., SF 01 to SF 05) cast slabs. A scatter in the values, recorded during experimentation and corresponding to each type of the slabs, is also shown in this table (i.e., Table 2). Further, typical stress–strain curves (one from each of the five different syntactic foam slabs cast) are shown in Fig. 2 where the often-stated two-stage [37] process is noticed. First stage represents high strength. This is followed by a second one where a plateau region is observed in accordance with a similar kind of report noted on syntactic foams having phenolic [37] and glass microballoons' [18]. The authors observed a distinct yield point in the stress–strain curve of glass microballoons bearing three-phase syntactic

Table 2 Effect of vol.% of microballoons on strength and modulus

Foam designation	Compressive strength (MPa)	Compressive modulus (MPa)
SF 01	82.4 ± 0.6	1627
SF 02	78.0 ± 0.5	1566.3
SF 03	69.6 ± 1	1445.6
SF 04	63.0 ± 1	1366.9
SF 05	58.0 ± 1	1336.4

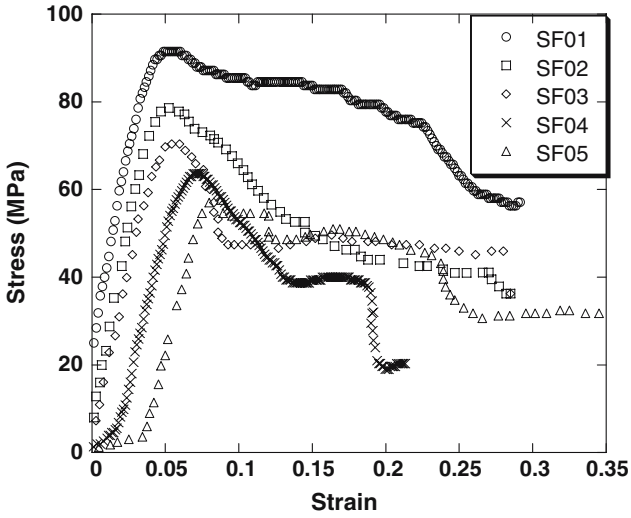

Fig. 2 Typical stress–strain curves for the five different syntactic foam slabs (i.e., SF 01 to SF 05)

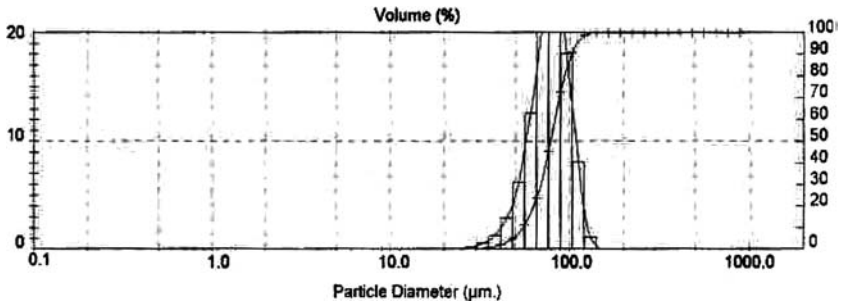

Fig. 1 A Graph revealing particle size distribution of glass hollow microspheres in terms of particle diameter and volume percentage of microballoons of that range

Table 3 One population *t*-test on different syntactic foam slabs at the 0.05 level

Foam designation	Mean	Variance	*N*	*t*	*p*
SF 01	82.4	1.1	5	0.21	0.84
SF 02	78.1	0.4	4	0.16	0.88
SF 03	69.6	2.6	4	0.46	0.67
SF 04	63.7	2.6	5	0.03	0.97
SF 05	58.1	1.4	6	0.35	0.74
SF 06	61.4	6.1	4	0.002	0.99

foams [18]. Stress–strain curves of all two-phase syntactic foams in this work also display the distinct yield point. Table 2, which is arrived at from the data in Fig. 2, when read along with Table 1, indicates that as volume % of microballoons increase the compressive yield strength decreases from slabs SF 01 to SF 05. To assure that the trends noticed are proper, a *t*-test was performed on the test data obtained on five samples each from SF 01 to SF 05 cases. The findings of such an effort are shown in Table 3. It indicates that for the 95% confidence limit the mean strength of SF 01 to SF 05 lies within the acceptable limit, hence the validation of the mean strength data at 0.05 level. Slope of the initial portion of Fig. 2 indicates the modulus of the slabs. It shows that as volume % of microballoons increase, the modulus decreases, as shown in Table 2. When the effects of density, which depends upon the filler content, on compressive yield strength and modulus were studied in PVC-rigid foam and PUR-rigid foam materials [38] a trend like the present one was noticed.

Effect of size distribution of microballoons

As stated earlier, vol.% of SF 06 added an additional variable in the present study, i.e., the cast slab had 40.1 vol.% of microballoons which is not replicated in any of the earlier cast (i.e., SF 01 to SF 05) slabs. The sample from SF 06 slab showed an experimentally determined strength value of 61.4 MPa that may be the outcome of at least two factors. First, the strength value recorded for this SF 06 is due to the microballoons content present in this slab and second, it would be reflecting the effect of size distribution of microballoons. To study which of the two is more appropriate, the strength data for 40.1 vol.% of microballoons was derived from the simple procedure of reading off the value based on the tabulated data presented in Table 2. This effort yielded a deduced value of 72.8 MPa (Fig. 3). This means that the strength corresponding to a slab of SF 06 type (i.e., the deduced value of the narrower size distribution of microballoons) is 18% higher compared to the experimentally determined value for the SF 06[b] (containing, as stated before, the broader sized distribution of microballoons). Additionally, the *t*-test analysis showed that for a 95% confidence limit the mean strength of SF 06 lies at 61.4 ± 2.91. Therefore, the experimental mechanical data of SF 06 are not overlapping with the deduced data. Hence, the validation of the data is at 0.05 level. This analysis points to the fact that the size distribution of microballoons has an effect on the strength.

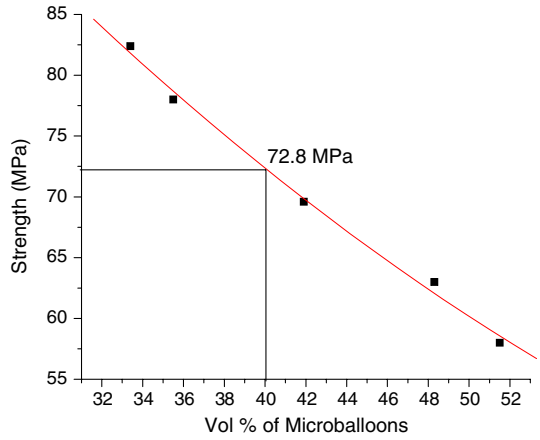

Fig. 3 Deducing the compressive strength value for a composition corresponding to the SF 06 (i.e., 40.1 vol.% bearing) case from the interpolation of strength versus volume percent of microballoons data

To observe the effect of size distribution of microballoons on modulus, data presented earlier in Table 2 is plotted as modulus versus volume percent of microballoons in Fig. 4. Following earlier adopted interpolation route, Fig. 4 gives modulus value of 1480.2 MPa for the narrower distribution case at 40.1 vol.% of microballoons. This shows that modulus of

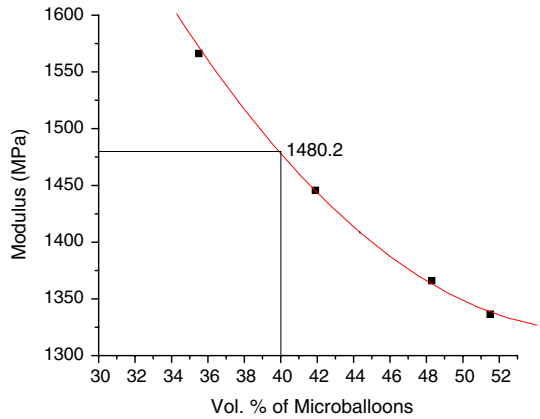

Fig. 4 Deducing the modulus value for a composition corresponding to the SF 06 case from the interpolation of modulus versus volume percent of microballoons data

the narrower (65–100 μm) size distribution case (i.e., 1480.2 MPa) is marginally higher than that for the samples having broader (i.e., 44–175 μm) distribution range which recorded a value of 1449.0 MPa. These findings show that size distribution of microballoons has a noticeable effect on compressive strength but for modulus, the effect is much less.

To check for the existence of any supporting results in literature, a search for the same was made from which it was noted that a similar trend on effect of particle size distribution is observed by Sidess et al. [39]. They pointed out that the ultimate properties (strength and strain) are much more sensitive to the mixture formulation due to their dependence on complete coverage of the filler by the matrix. On the other hand, the intrinsic properties like density and modulus are less sensitive as they depend on better compaction and bridging phenomenon [39].

Microscopy

To explain the mechanical data regarding the effect of microballoons content on strength, microscopic examination was done at different magnifications. Microscopy was done first for the samples displaying lowest strengths (SF 05) followed by those having intermediate values (SF 03) and finally for the coupons made from the slabs having maximum strength (SF 01). Figure 5 is a lower magnification micrograph taken on one of the samples showing least strength, where complete crushing and collapsing of microballoons can be seen all over the surface and matrix deformation marks are difficult to locate due to the spread of the debris. A crushed microballoon can be seen in the bottom right corner of this figure, i.e., Fig. 5. These findings indicate that due to the large volume of microballoons and the attendant load-bearing ability of the system being affected, the sample exhibits the least strength. Figure 6 represents the micrograph of the intermediate strength case, where the surfaces of both the microballoons, visible in the photograph (and marked 1 & 2), display cracked features. However, collapse of the microballoons, seen earlier in Fig. 5, is not easy to recognize. Instead, in both the microballoons, multi segmentally cracked features are seen. Further, matrix around microballoons, especially the one positioned at the top display deformation marks, which were difficult to notice in the least strength case partly because of spread debris (Fig. 5). Microscopy of the highest strength case is shown in Fig. 7. This shows multiple fracturing of the microballoons, marked as 1, whose intensity is more compared to the intermediate strength case (i.e., Fig. 6), discussed earlier. Also, a darkened curvilinear crack propagating in the matrix-bearing region from the top right portion to the bottom right portion of the micrograph can clearly be seen. Around the central microballoon and on the right side of the photograph the matrix deformation marks can

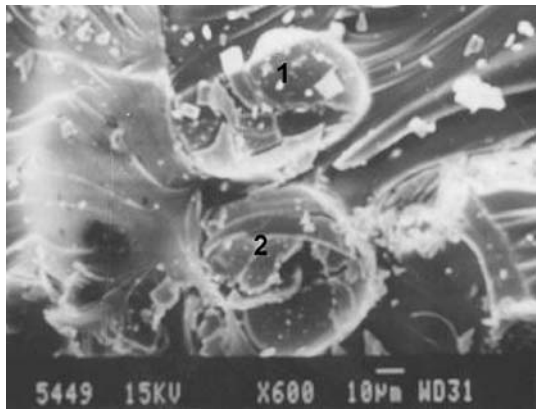

Fig. 6 The micrograph of a test coupon from the intermediate strength-bearing slab (i.e., SF 03) case displaying multi-segment cracking of the microballoons marked 1 and 2

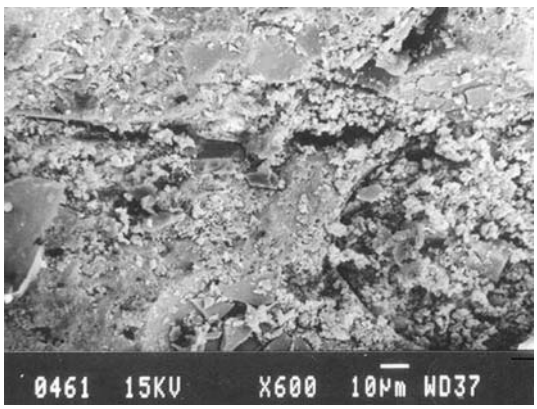

Fig. 5 Low magnification micrograph of the least strength-bearing slab (i.e., SF 05) displaying complete crushing of microballoons in the bottom right corner

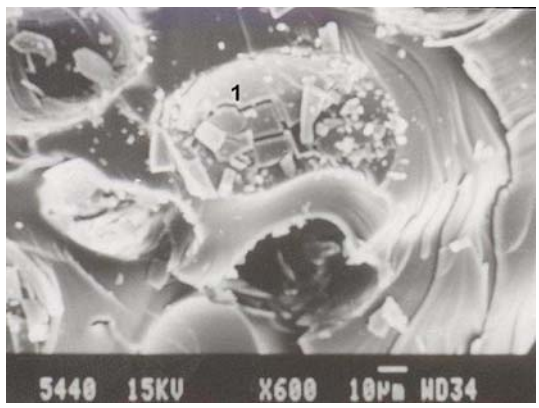

Fig. 7 Low magnification micrograph of the highest strength-bearing slab (i.e., SF 01) showing multiple fracturing of the microballoons (marked 1)

be seen in Fig. 7. These microscopic features illustrate the fact that in highest strength case (SF 01), fracture features are dominated by the matrix deformation while, as stressed earlier, in the least strength case, (i.e., SF 05) failure of the sample is related to collapsing and caving-in-like features for the microballoons.

To correlate the mechanical data with microscopic features better, further microscopic examination was done at a still higher magnification, and the resulting efforts are presented in the sets of figures, i.e., Figs. 8–12 for the three levels of strengths of samples discussed earlier. Thus, Figs. 8 and 9 are the (higher magnification) micrographs taken at two locations for the least strength case (SF 05). A completely crushed, collapsed and caved-in microballoon can be clearly seen in the center of Fig. 8 while Fig. 9 shows a portion of the matrix that is sandwiched amongst the microballons visible clearly in the photograph, which in this chosen area, has least debris scattered on them. This region lies within the four microballoons numbered 1–4 at the four corners of the photograph. Crushing features can be seen prominently in the microballoons marked 1 and 3. Also some less distinct deformation marks on the matrix in the center part of the micrograph are seen. This feature was difficult to study at lower magnifications owing to debris. Figure 10 is a micrograph taken on the intermediate strength bearing sample case (SF 03). This shows more matrix deformation marks compared to the ones seen in Fig. 9. Figures 11 and 12 are the micrographs taken for the highest strength, that is, the least microballoons-bearing sample. Of these, the feature in Fig. 11 shows multiple cracking of the microballoon (marked as 1). Prominent curvilinear deformation marks of the matrix can be seen to the right of this fragmented microballoons in this photograph. Figure 12 shows extensive multiple cracking of the two microballoons marked as 1 and 2. Also, matrix deformation marks, emphasizing presence of shear conditions, are clearly visible in Fig. 12. All these features point to the fact that in the least microballoons case the load-bearing component is the matrix and hence strengths and modulus of the samples are high while in highest microballoons case the collapse of

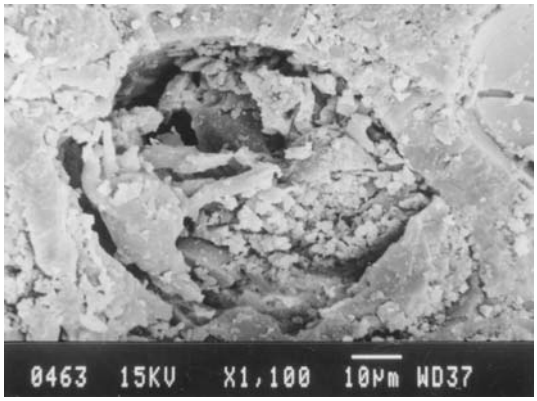

Fig. 8 A photograph illustrating the complete crushing and collapsing of the microballoon positioned in the center of the micrograph for the least strength-bearing slab (i.e., SF 05)

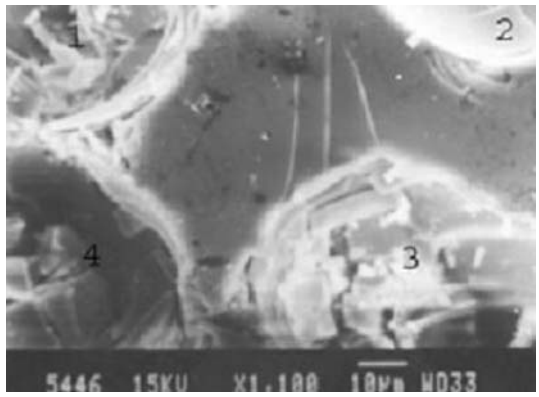

Fig. 9 The matrix sandwiched amongst four microballoons (marked 1–4) showing less distinct deformation marks in the center of the micrograph

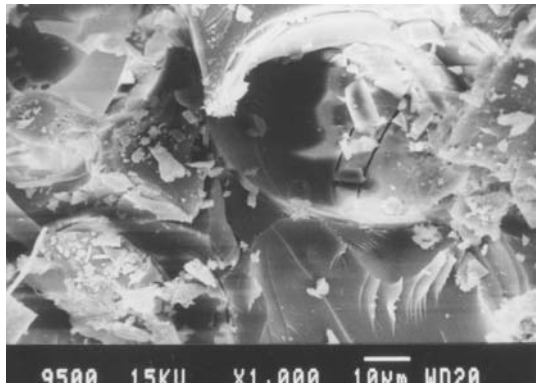

Fig. 10 Intermediate strength-bearing sample (i.e., SF 03) showing matrix deformation marks in the right bottom region of the photograph

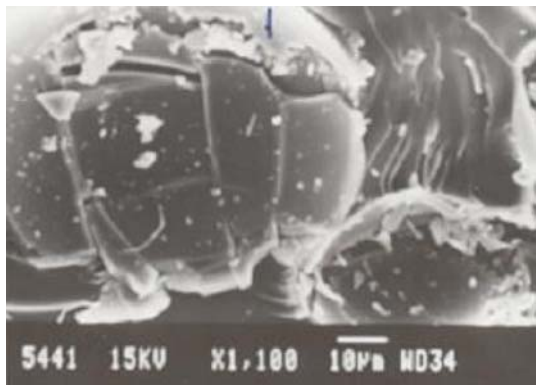

Fig. 11 Multiple cracking of the microballoons both in the longitudinal and transverse directions for the highest strength bearing slab (SF 01)

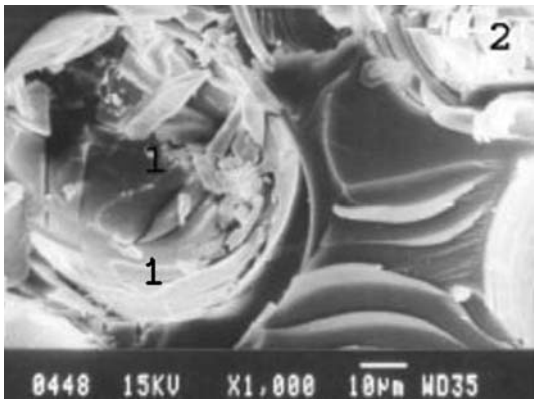

Fig. 12 Another micrograph of the highest strength-bearing slab (SF 01) showing prominent curvilinear deformation marks in the right-hand region of the micrograph

microballoons leads to a lowering of both these compression test values.

Conclusion

It is evident from the present study that as the volume percent of the microballoons increases, density of the foam, compressive strength and modulus decreases. Syntactic foam having least microballoons content shows prominent matrix deformation marks and multiple fracturing of microballoons while foams with highest microballoons content reveals crushing and caving-in of microballoons. Also evident from this approach is the fact that compressive strength is somewhat higher for the narrower distribution of microballoons case, having an average particle size of 82 μm, compared to the broader distribution case, with an average particle size of 109 μm.

Acknowledgements The authors acknowledge the contributions of Messrs. Jagdish, Ravi Sekhar and Govind Raju of ADE who were involved in the preparation of the syntactic foams. The first (K) and second (RS) authors are grateful to Mr. Sasidhara for his help in conducting the compression tests. The first author (K) further would like to place on record the assistance rendered by the members of the Polymer Composites Laboratory in the Department of Metallurgy at various stages of the work.

References

1. Hall CK (April 1984) In Proc of Conf On FRP. University of Liverpool, UK
2. Narkis M, Putterman M, Keing S (1983) In: SPI, 38th Annual conference by Reinforced Plastics/Composites Institute, 'Composite Solutions to Materials'. Society of the Plastics Industry, Houston, Texas, USA Sess, 8fp, 2
3. Rand PB (1978) J Cellu Plast 14:277
4. Benning CJ (1969) In: Plastic Foams, vol 1. John Wiley, New York, p 537
5. Huttinger KJ (1971) Carbon 9:222
6. Volk MC (1969) Encyclopedia of Polym Sci Technol, vol 8, Reinhold, New York, p 752
7. Braun T, Frag AB (1978) Anal Chem Acta 99:1
8. Shutov FA (1986) Adv Polym Sci 63:73
9. Kishore, Shankar R, Sankaran S (2005) Mater Sci Eng A 412:153
10. Gibson LJ, Wegner LD (1994) Cellular Microcellular Mater ASME 53:83
11. Gibson LJ, Ashby MF (1997) In: Cellular solids: structure and properties, 2nd ed. Cambridge University Press, New York, p 345
12. Rittel D (2005) Mater Lett 59:1845
13. Song B, Chen W, Frew DJ (2004) J Compos Mater 38:915
14. Wouterson EM, Boey FYC, Hu X, Wong S-C (2004) J Cellu Plast 40:145
15. Bardella L, Genna F (2001) Intl J Solid Struct 38:7235
16. Rizzi E, Papa E, Corigliano A (2000) Compos Sci Technol 60:2169
17. Lawrence E, Pyrz R (2001) Polym Polym Compos 9:227
18. Gupta N, Kishore, Woldesenbet E, Sankaran S (2001) J Mater Sci 36:4485
19. Rizzi E, Papa E, Corigliano A (2000) Int J Solid Struct 37:5773
20. Kim HS, Plubrai P (2004) Compos Part A 35:1009
21. Woldesenbet E, Gupta N, Jerro HD (2005) J Sand Struc Mater 7:95
22. Karthikeyan CS, Sankaran S, Kishore (2004) Mater Lett 58:995
23. Gupta N, Woldesenbet E, Mensah P (2004) Compos Part A 35:103
24. Wouterson EM, Boey FYC, Hu X, Wong S-C (2005) Compos Sci Technol 65:1840
25. Marur PR (2005) Mater Lett 59:1954
26. Gupta N, Woldesenbet E (2004) J Cell Plast 40:461
27. El-Hadek A, Tippur HV (2002) J Mater Sci 37:1649
28. Huang Y-J, Vaikhanski L, Nutt SR Compos. Part A, corrected proof available online 22 July 2005
29. Gupta N, Woldesenbet E (November, 2002) In: Proc SAMPE Symp, Baltimore, p 4
30. Kishore, Shankar R, Sankaran S (2005) J Appl Polym Sci 98:680
31. Kishore, Shankar R, Sankaran S (2005) J Appl Polym Sci 98:687
32. Kim HS, Plurai P (July, 2002) In: Proc Australian conference on composites, ACUN–4, Composite Systems, Sydney, p 21
33. Bruneton E, Tallaron C, Gras-Naulin N, Cosculluela A (2002) Carbon 40:1919
34. Kenig S, Raiter I, Narkis M (1984) J Cell Plast 20:423
35. Okuno K, Woodhams RT (1974) J Cell Plast 10:237
36. ASTM D 1621–73, Standard test method for compressive properties of rigid cellular plastics
37. Bunn P, Mottram JT (1993) Compos 24:565
38. Menges G, Knipschild F (1982) In: Hylyard NC (ed) Mechanics of cellular plastics, Ch. 2A. Appl Sci Pub, Essex, England, p 67
39. Sidess A, Holdengraber Y, Buchman A (1993) Compos 24:355